

Hydroxopalladium(IV) Complexes Prepared Using Oxygen or Hydrogen Peroxide as Oxidants

Supporting Information

Ava Behnia, Mahmood A. Fard, Johanna M. Blacquiere* and Richard J. Puddephatt*

Department of Chemistry, University of Western Ontario, London, Canada N6A 5B7

Table of Contents

I – NMR Spectra	S2
II – Crystallographic Details	S9
III – DFT Figures	S13
IV – References	S15

I – NMR Spectra

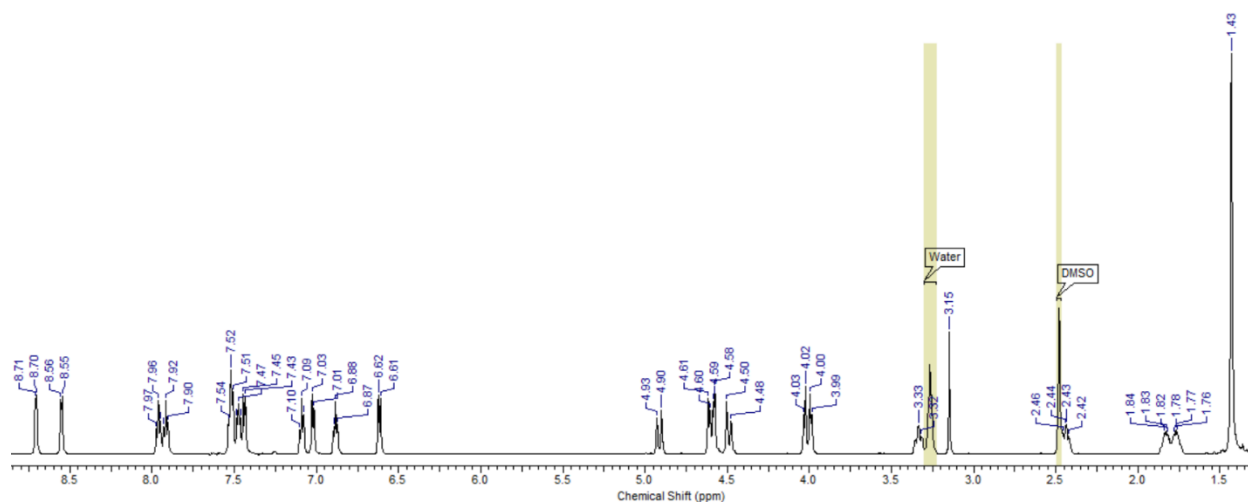


Figure S1. ^1H NMR spectrum of $[\text{Pd}^{\text{IV}}(\text{CH}_2\text{CMe}_2\text{C}_6\text{H}_4)(\kappa^3\text{-N,N',N''-L1})\text{OH}][\text{PF}_6]$, **3**, in $(\text{CD}_3)_2\text{SO}$, at 25 °C, 600 MHz.

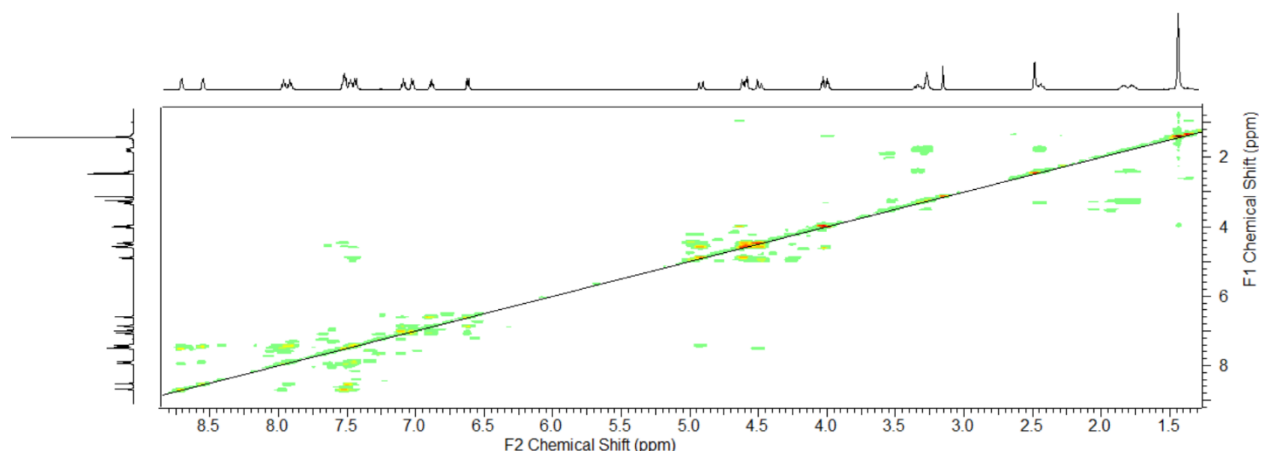


Figure S2 ^1H - ^1H COSY spectrum of $[\text{Pd}^{\text{IV}}(\text{CH}_2\text{CMe}_2\text{C}_6\text{H}_4)(\kappa^3\text{-N,N',N''-L1})\text{OH}][\text{PF}_6]$, **3**, in $(\text{CD}_3)_2\text{SO}$, at 25°C.

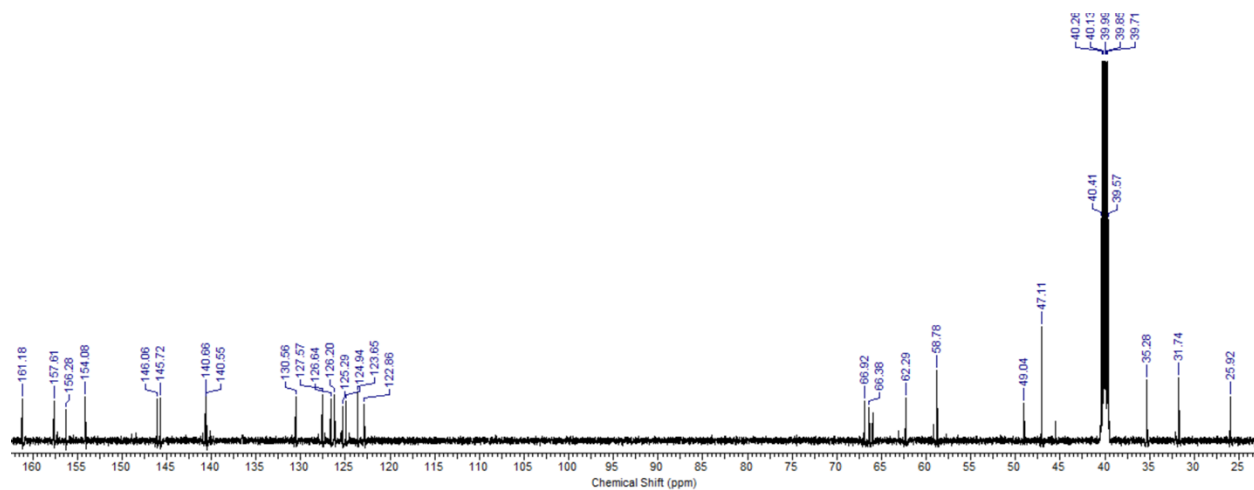


Figure S3. $^{13}\text{C}\{^1\text{H}\}$ NMR spectrum of $[\text{Pd}^{\text{IV}}(\text{CH}_2\text{CMe}_2\text{C}_6\text{H}_4)(\kappa^3\text{-N,N',N''-L1})\text{OH}][\text{PF}_6]$, **3**, in $(\text{CD}_3)_2\text{SO}$, at $25\text{ }^\circ\text{C}$, 151 MHz.

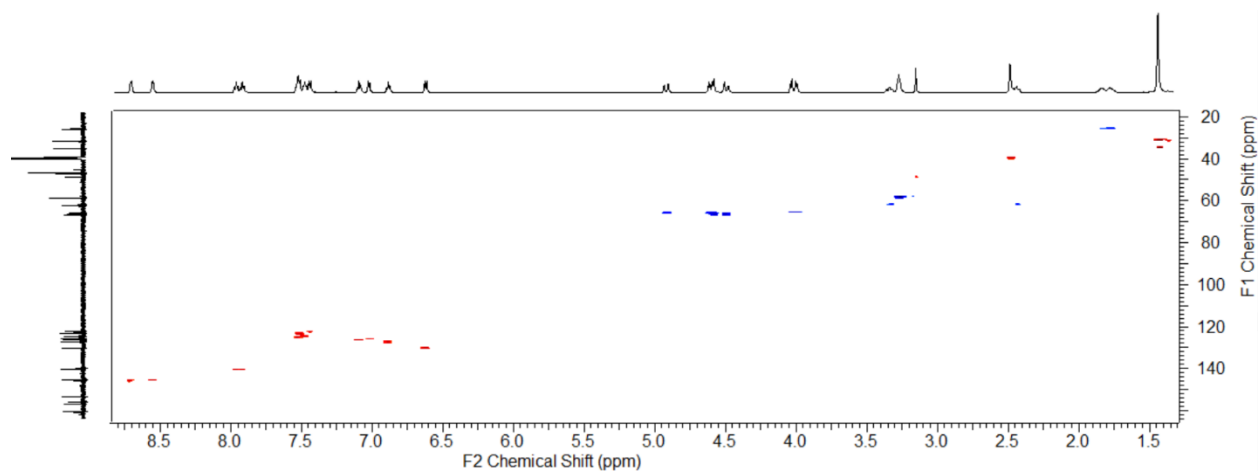


Figure S4. ^1H - ^{13}C HSQC spectrum of $[\text{Pd}^{\text{IV}}(\text{CH}_2\text{CMe}_2\text{C}_6\text{H}_4)(\kappa^3\text{-N,N',N''-L1})\text{OH}][\text{PF}_6]$, **3**, in $(\text{CD}_3)_2\text{SO}$, at $25\text{ }^\circ\text{C}$.

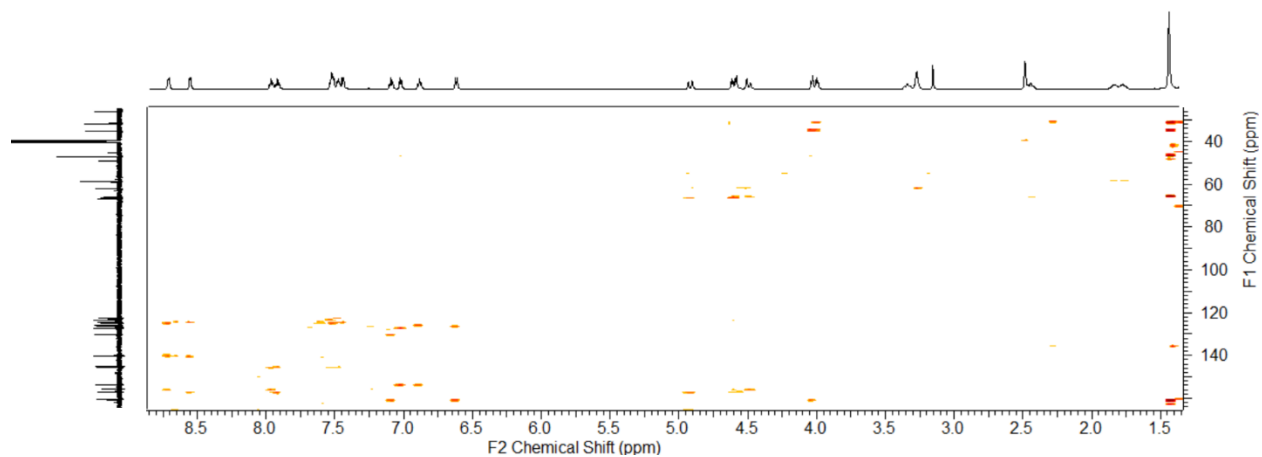


Figure S5. ^1H - ^{13}C HMBC spectrum of $[\text{Pd}^{\text{IV}}(\text{CH}_2\text{CMe}_2\text{C}_6\text{H}_4)(\kappa^3\text{-N,N',N''-L1})\text{OH}][\text{PF}_6]$, **3**, in $(\text{CD}_3)_2\text{SO}$, at $25\text{ }^\circ\text{C}$.

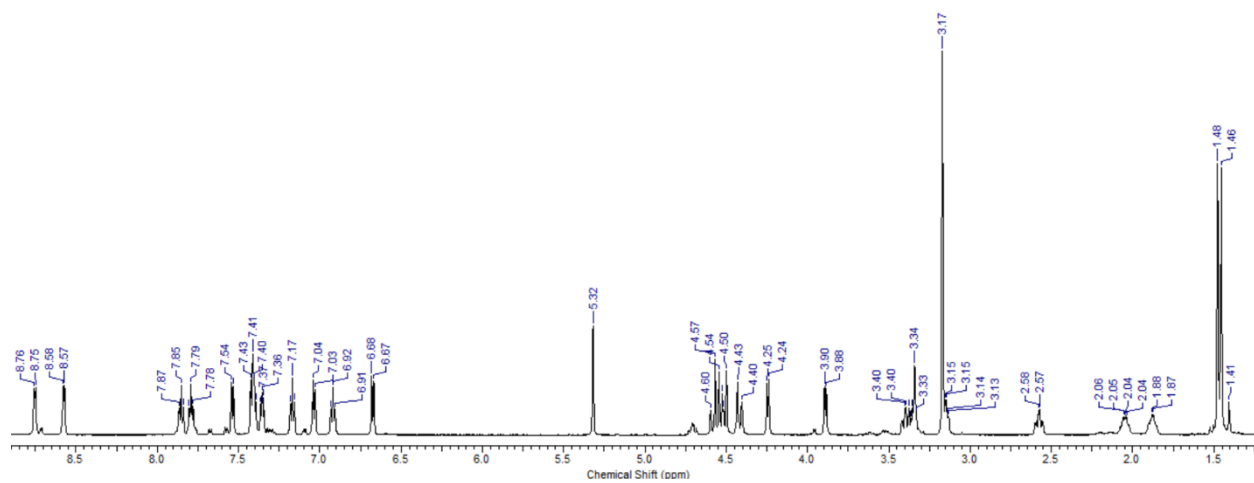


Figure S6. ^1H NMR spectrum of $[\text{Pd}^{\text{IV}}(\text{CH}_2\text{CMe}_2\text{C}_6\text{H}_4)(\kappa^3\text{-N,N',N''-L2})\text{OH}][\text{PF}_6]$, **4**, in CD_2Cl_2 , at $-10\text{ }^\circ\text{C}$, 600 MHz.

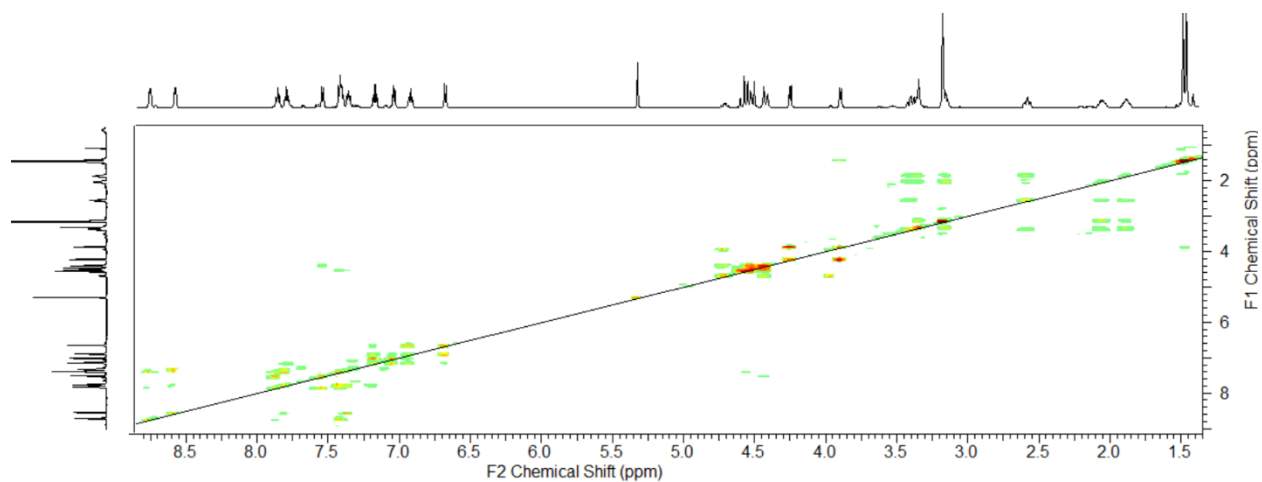


Figure S7. ^1H - ^1H COSY spectrum of $[\text{Pd}^{\text{IV}}(\text{CH}_2\text{CMe}_2\text{C}_6\text{H}_4)(\kappa^3\text{-N,N',N''-L2})\text{OH}][\text{PF}_6]$, **4**, in CD_2Cl_2 , at $-10\text{ }^\circ\text{C}$.

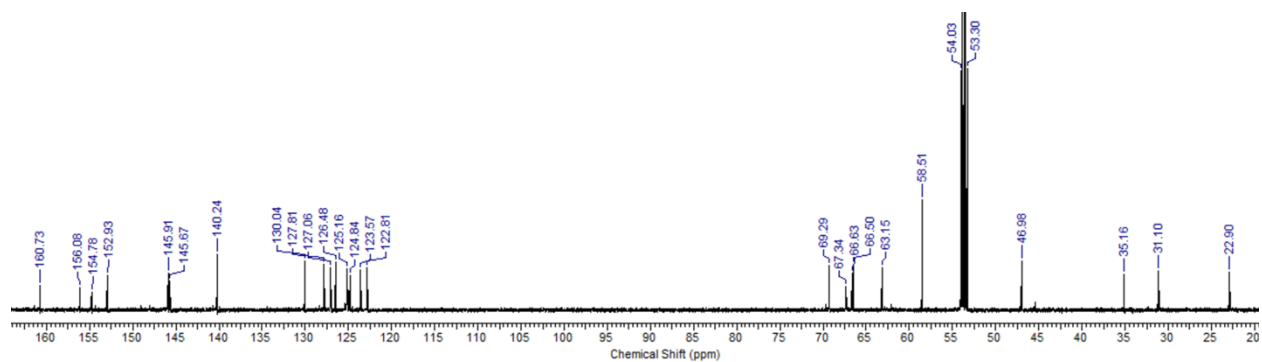


Figure S8. $^{13}\text{C}\{^1\text{H}\}$ spectrum of $[\text{Pd}^{\text{IV}}(\text{CH}_2\text{CMe}_2\text{C}_6\text{H}_4)(\kappa^3\text{-N,N',N''-L2})\text{OH}][\text{PF}_6]$, **4**, in CD_2Cl_2 , at $-10\text{ }^\circ\text{C}$, 151 MHz.

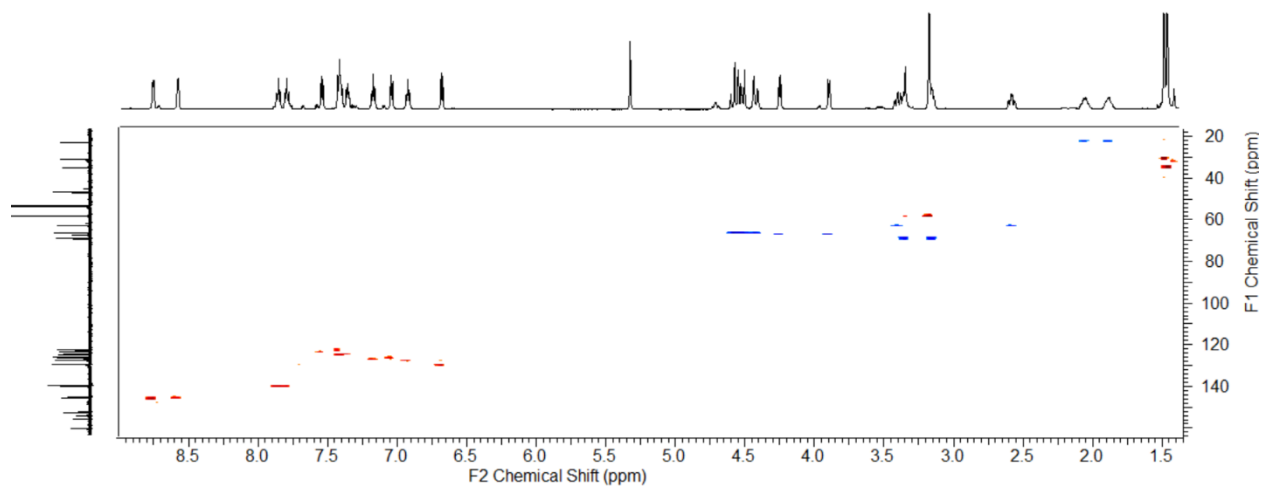


Figure S9. ^1H - ^{13}C HSQC spectrum of $[\text{Pd}^{\text{IV}}(\text{CH}_2\text{CMe}_2\text{C}_6\text{H}_4)(\kappa^3\text{-N,N',N''-L2})\text{OH}][\text{PF}_6]$, **4**, in CD_2Cl_2 , at $-10\text{ }^\circ\text{C}$.

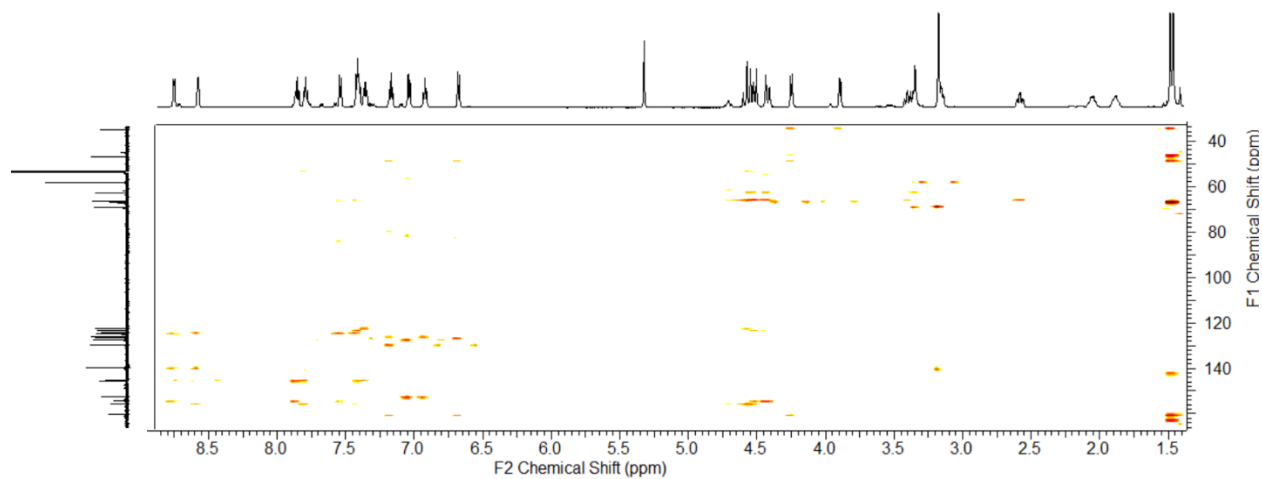


Figure S10. ^1H - ^{13}C HMBC spectrum of $[\text{Pd}^{\text{IV}}(\text{CH}_2\text{CMe}_2\text{C}_6\text{H}_4)(\kappa^3\text{-N,N',N''-L2})\text{OH}][\text{PF}_6]$, **4**, in CD_2Cl_2 , at $-10\text{ }^\circ\text{C}$.

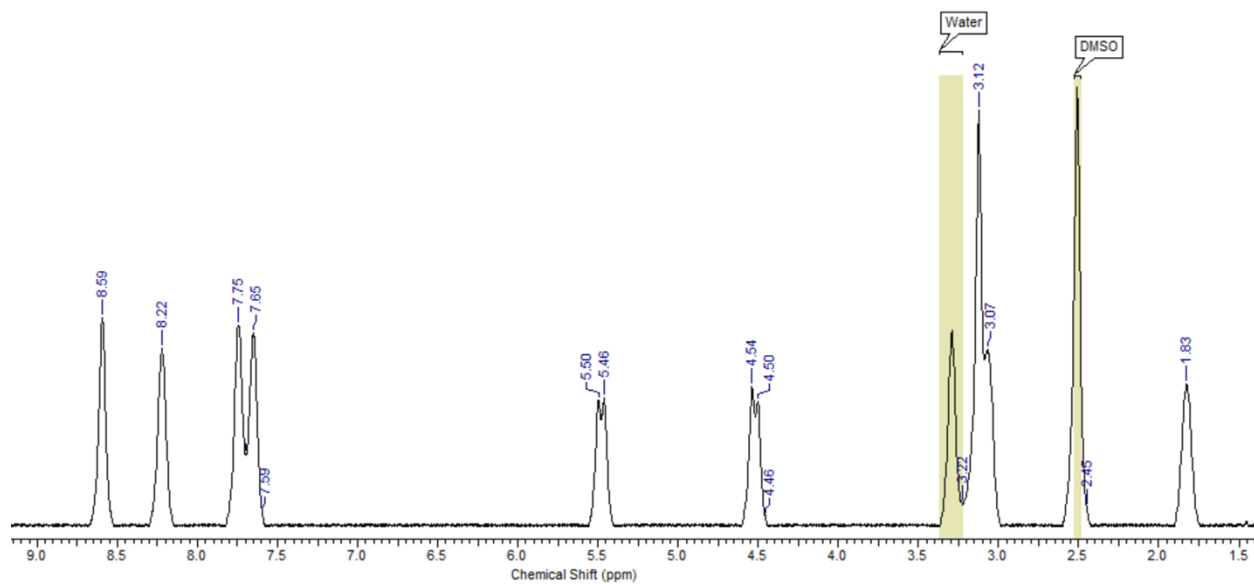


Figure S11. ^1H NMR spectrum of $[\text{Pd}^{\text{IV}}(\text{CH}_2\text{CMe}_2\text{C}_6\text{H}_4)(\kappa^3\text{-N,N',N''-L2})\text{OH}][\text{PF}_6]$, **4**, in $(\text{CD}_3)_2\text{SO}$, at 25 °C, 600 MHz.

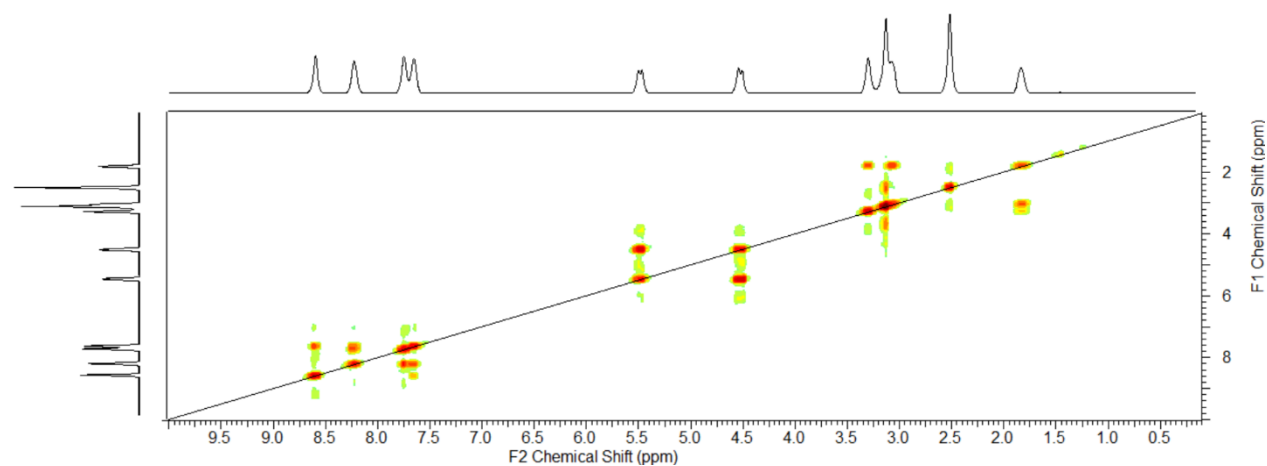


Figure S12. ^1H - ^1H COSY spectrum of $[\text{Pd}^{\text{IV}}(\text{CH}_2\text{CMe}_2\text{C}_6\text{H}_4)(\kappa^3\text{-N,N',N''-L2})\text{OH}][\text{PF}_6]$, **4**, in $(\text{CD}_3)_2\text{SO}$, at 25 °C.

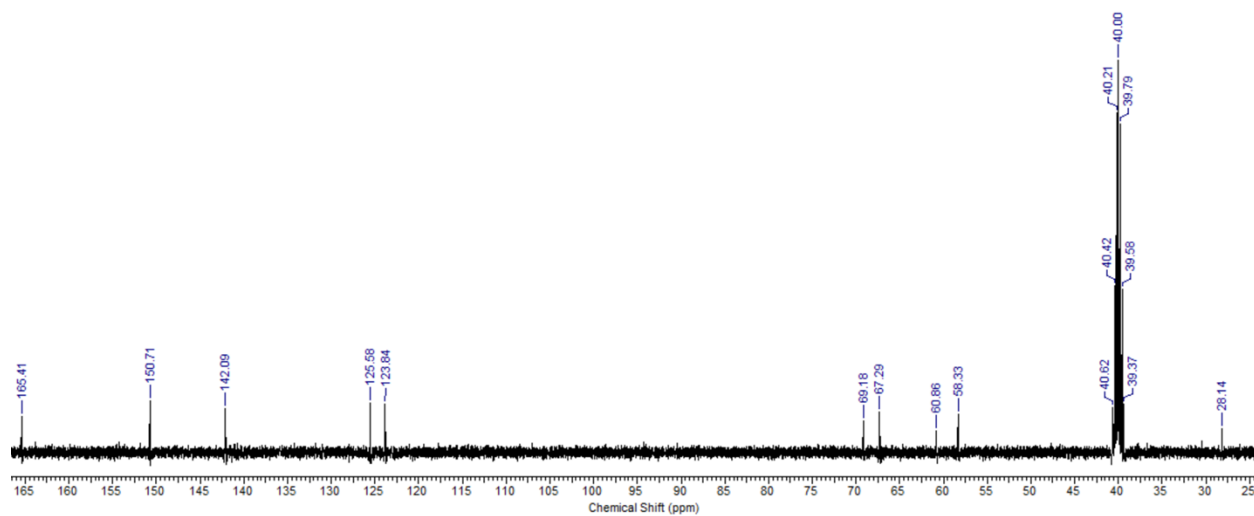


Figure S13. $^{13}\text{C}\{^1\text{H}\}$ NMR spectrum of $[\text{Pd}^{\text{IV}}(\text{CH}_2\text{CMe}_2\text{C}_6\text{H}_4)(\kappa^3\text{-N,N',N''-L2})\text{OH}][\text{PF}_6]$, **4**, in $(\text{CD}_3)_2\text{SO}$, at 25 °C, 151 MHz.

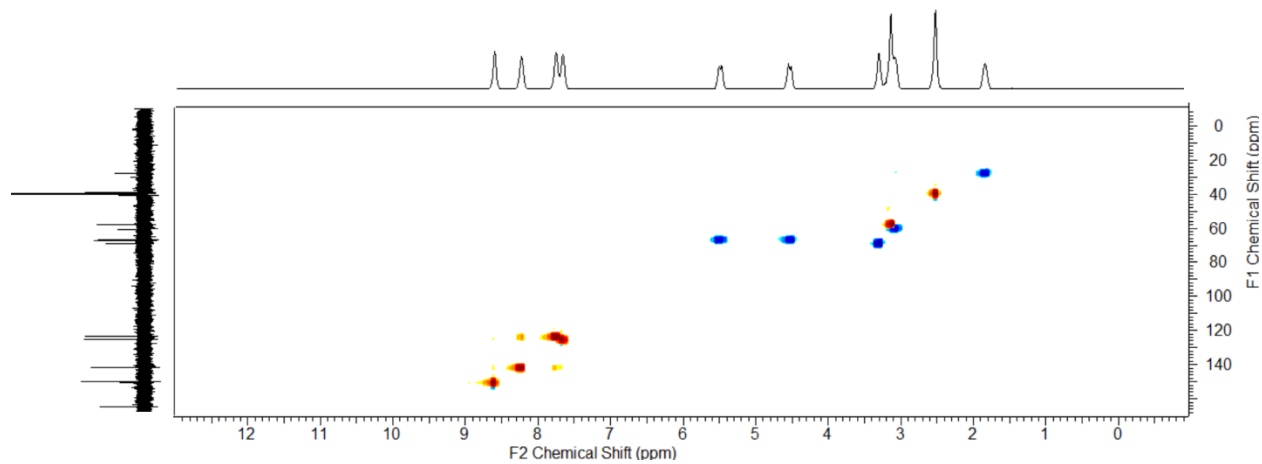


Figure S14. ^1H - ^{13}C HSQC spectrum of $[\text{Pd}^{\text{IV}}(\text{CH}_2\text{CMe}_2\text{C}_6\text{H}_4)(\kappa^3\text{-N,N',N''-L2})\text{OH}][\text{PF}_6]$, **4**, in $(\text{CD}_3)_2\text{SO}$, at 25 °C.

II – Crystallographic Details

Data Collection and Processing. The sample was mounted on a Mitegen polyimide micromount with a small amount of Paratone N oil. All X-ray measurements were made on a Bruker Kappa Axis Apex2 diffractometer at a temperature of 110 K. The frame integration was performed using SAINT.¹ The resulting raw data was scaled and absorption corrected using a multi-scan averaging of symmetry equivalent data using SADABS.²

Structure Solution and Refinement. The structures were solved by using a dual space methodology using the SHELXT program.³ All non-hydrogen atoms were obtained from the initial solution. The hydrogen atoms were introduced at idealized positions and were allowed to ride on the parent atom. The structural model was fit to the data using full matrix least-squares based on F^2 . The calculated structure factors included corrections for anomalous dispersion from the usual tabulation. The structure was refined using the SHELXL program from the SHELXTL suite of crystallographic software.⁴ Graphic plots were produced using the Mercury program suite.⁵

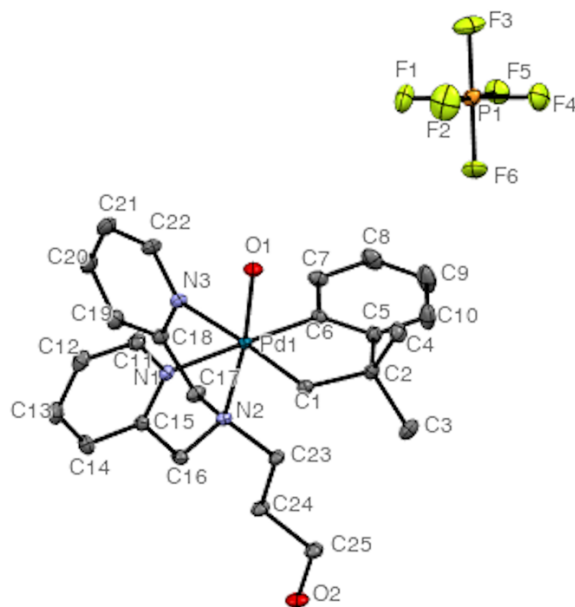


Figure S15. Displacement ellipsoid plot of **3** showing naming and numbering scheme. Ellipsoids are drawn at the 50% probability level and hydrogen atoms are omitted for clarity.

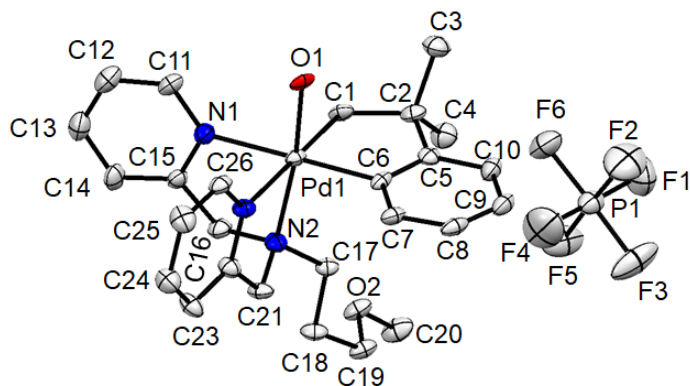


Figure S16. Displacement ellipsoid plot of **4** showing naming and numbering scheme. Ellipsoids are drawn at the 50% probability level and hydrogen atoms are omitted for clarity.

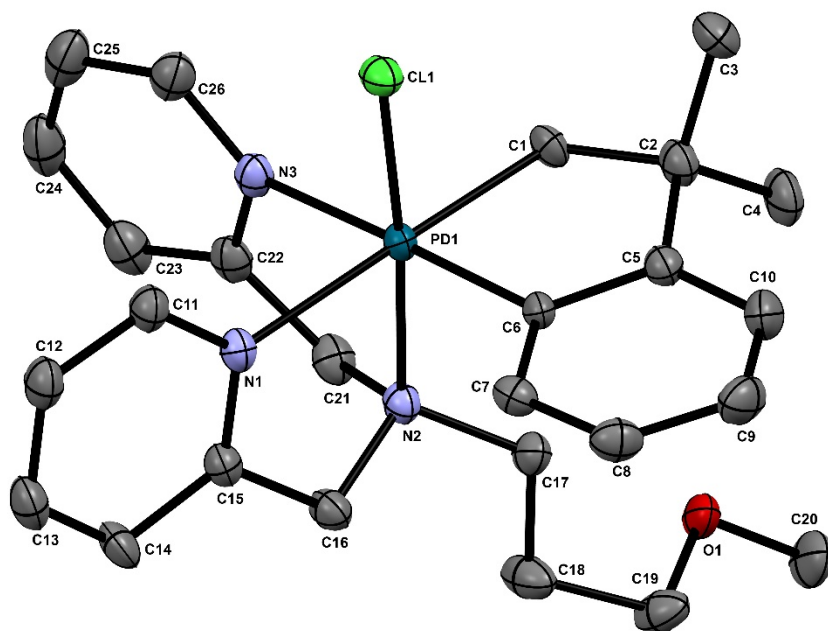


Figure S17. The structure of complex **7**, showing 50% probability ellipsoids.

Table S1. Crystallographic data and parameters for compounds **3** and **4**.

Compound Number (CCDC)	3 (2091354)	4 (2091353)	7 (2334979)
Formula	C ₂₅ H ₃₂ F ₆ N ₃ O ₂ PPd	C ₂₆ H ₃₄ N ₃ O ₂ PPd	C ₂₆ H ₃₃ ClF ₆ N ₃ OPPd
Formula weight (g/mol)	657.93	671.96	690.37
Crystal system	Monoclinic	Orthorhombic	Orthorhombic
Space group	P 2 ₁ /n	P 2 ₁ 2 ₁ 2 ₁	P 2 ₁ 2 ₁ 2 ₁
<i>a</i> [Å]	11.154(4)	10.060(4)	10.359(4)
<i>b</i> [Å]	10.056(5)	13.2520(6)	13.204(7)
<i>c</i> [Å]	23.767(11)	20.6558(9)	20.622(9)
<i>α</i> [°]	90	90	90
<i>β</i> [°]	92.48(3)	90	90
<i>γ</i> [°]	90	90	90
<i>V</i> [Å ³]	2663(2)	2753.9 (16)	2821(2)
<i>Z</i>	4	4	4
Min and Max 2θ for cell determination, [°]	5.32, 72.18	2.50, 31.67	2.20, 30.41
<i>F</i> (000)	1336	1368	1400
<i>ρ</i> (g/cm ³)	1.641	1.621	1.626
<i>λ</i> , Å, (MoKα)	0.71073	0.71073	0.71073
Number of reflections measured	96056	70130	58116
Number of unique reflections	12720	9305	9536
<i>R</i> ₁	0.0251	0.0800	0.0422
w <i>R</i> ₂ [<i>I</i> ≥ 2σ(<i>I</i>)]	0.0586	0.1959	0.0505

R_1 (all data)	0.0322	0.0979	0.0904
wR_2 (all data)	0.0613	0.2080	0.0938
GOF	1.021	1.024	0.999
Maximum shift/error	0.001	0.0001	0.002
Min & Max peak heights on final ΔF Map ($e^-/\text{\AA}$)	-1.008, 0.708	-2.056, 3.465	-2.232, 1.553

Where:

$$R_1 = \sum (|F_o| - |F_c|) / \sum F_o$$

$$wR_2 = [\sum (w(F_o^2 - F_c^2)^2) / \sum (w F_o^4)]^{1/2}$$

$$GOF = [\sum (w(F_o^2 - F_c^2)^2) / (\text{No. of reflns.} - \text{No. of params.})]^{1/2}$$

III – DFT Figures

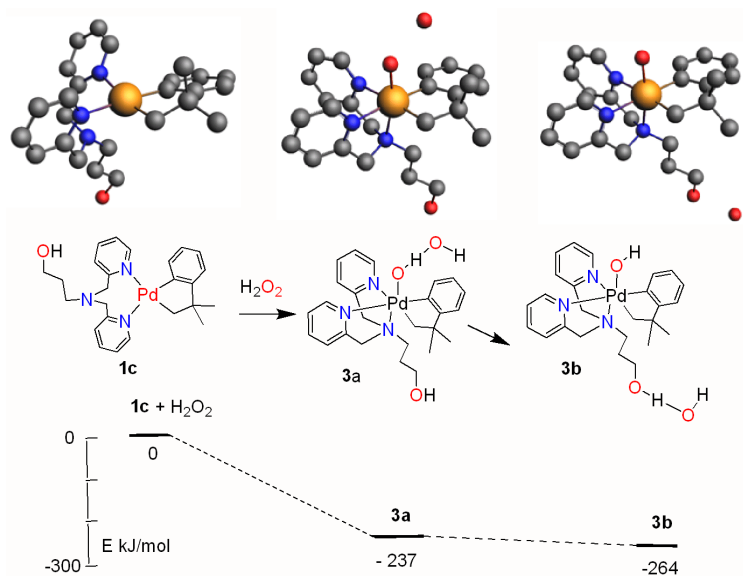


Figure S18. The calculated structures and relative energies, with respect to **1c** + H_2O_2 , of complexes **3a** and **3b**.

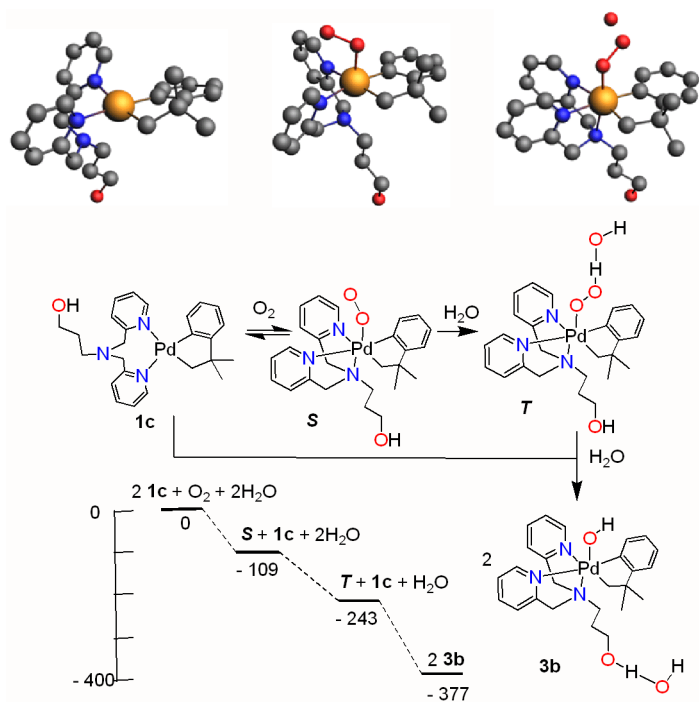


Figure S19. The calculated structures and energies (kJ/mol with respect to $2\text{1c} + \text{O}_2 + 2\text{H}_2\text{O}$) of complexes formed by reaction of complex **1** with dioxygen.

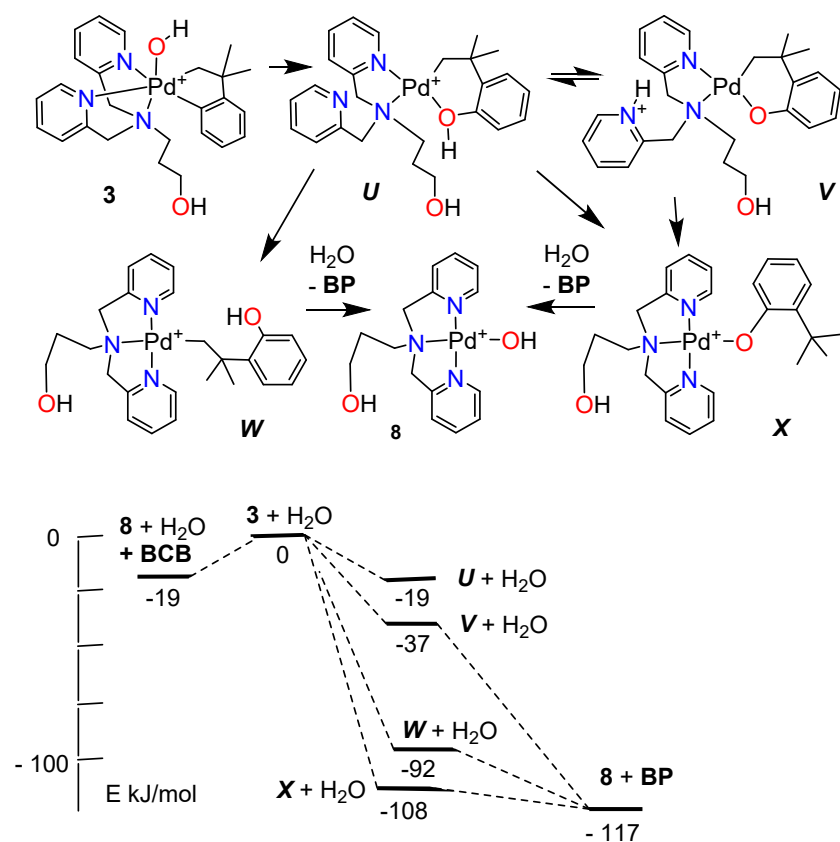


Figure S20. Possible mechanisms of reductive elimination from complex **3** and the calculated relative energies (E kJ mol⁻¹) of potential intermediates and products.

IV - References

1. Bruker-Nonius; SAINT; version; 2013.8, **2013**, Bruker-Nonius, Madison, WI 53711, USA
2. Bruker-Nonius; SADABS; version; 2012.1, **2012**, Bruker-Nonius, Madison, WI 53711, USA.
3. Sheldrick, G., SHELXT - Integrated space-group and crystal-structure determination. *Acta Crystallogr. Sect. A* **2015**, *A71*, 3-8.
4. Sheldrick, G., Crystal structure refinement with SHELXL. *Acta Crystallogr. Sect. C* **2015**, *C71*, 3-8.
5. Macrae, C. F.; Bruno, I. J.; Chisholm, J. A.; Edgington, P. R.; McCabe, P.; Pidcock, E.; Rodriguez-Monge, L.; Taylor, R.; van de Streek, J.; Wood, P. A., Mercury CSD 2.0 - new features for the visualization and investigation of crystal structures. *J. Appl. Cryst.* **2008**, *41*, 466-470.